RSC Advances

PAPER

View Article Online
View Journal | View Issue

Cite this: *RSC Adv.*, 2023, **13**, 10592

Insight into the interaction between tannin acid and bovine serum albumin from a spectroscopic and molecular docking perspective

Wei Xu, *[a] Yuli Ning,[a] Shiwan Cao,[a] Guanchen Wu,[a] Haomin Sun,[b] Liwen Chai,[b] Shuping Wu, [b] Jingyi Li[a] and Denglin Luo[b]

In this study, the interaction mechanism of bovine serum albumin (BSA) with tannic acid (TA) was investigated by spectroscopic and computational approaches and further validated using circular dichroism (CD), differential scanning calorimetry (DSC) and molecular docking techniques. The fluorescence spectra showed that TA bound to BSA and underwent static quenching at a single binding site, which was consistent with the molecular docking results. And the fluorescence quenching of BSA by TA was dose-dependent. Thermodynamic analysis indicated that hydrophobic forces dominated the interaction of BSA with TA. The results of circular dichroism showed that the secondary structure of BSA was slightly changed after coupling with TA. Differential scanning calorimetry showed that the interaction between BSA and TA improved the stability of the BSA–TA complex, and the melting temperature increased to 86.67 °C and the enthalpy increased to 264.1 J g^{-1} when the ratio of TA to BSA was 1.2 : 1. Molecular docking techniques revealed specific amino acid binding sites for the BSA–TA complex with a docking energy of −12.9 kcal mol^{-1}, which means the TA is non-covalently bound to the BSA active site.

Received 18th January 2023
Accepted 20th March 2023

DOI: 10.1039/d3ra00375b

rsc.li/rsc-advances

1 Introduction

Tannin acid (TA) is a high molecular weight water-soluble polyphenol that has been widely used as a food additive in recent years. It has excellent antibacterial activity and free radical scavenging ability, and is used as a natural preservative in the food industry.[1,2] Due to its unique physiological activity and medicinal value, it is widely used as a medicine to prevent and treat diseases, such as hemostasis, inhibition of microbial growth, anti-allergy, anti-tumor, anti-aging, *etc.*[3] The pharmacological activity of TA has excellent potential for development and application.[4,5] TA molecules contain reactive functional groups, such as phenolic hydroxyl, hydroxyl and carboxyl groups, which can form complexes with proteins, polysaccharides, alkaloids and nucleic acids.[6] It is important to study the mechanism of TA binding to proteins and the application of their complexes in functional foods.

In recent years, proteins have been widely used as carriers for stabilization and delivery of active molecules due to their unique chemical structure and multiple functional properties. Studies on the interaction of bioactive molecules with human serum albumin have recently been carried out to gain accurate insight into the use of bioactive molecules in the food and pharmaceutical industries.[7,8] Moreover, bovine serum albumin (BSA) is one of the most studied proteins, mainly due to its high homology (~76%) and similar 3D structure to human serum albumin.[9] In addition, the molecular structure of BSA has many accessible free carboxyl and amino groups as well as various binding sites. This makes it easier to bind to active molecules and to form stable complexes with various endogenous and exogenous compounds such as ions, fatty acids, drug molecules and toxic exogenous compounds.[10,11] It has a transport function and is responsible for delivering endogenous or exogenous molecules to their targets.[12] The formation of high-affinity albumin-ligand complexes can influence membrane transport, distribution and elimination of ligand molecules.[13]

BSA is a non-specific transporter protein that binds to small molecules such as TA that enter the body to form complexes. They are circulated to target spot where they can exert their effects.[14,15] Jia *et al.* investigated the interaction mechanism of chlorogenic acid (CGA) with BSA using UV-vis spectroscopy, fluorescence spectroscopy, circular dichroism, molecular dynamics simulations and cyclic voltammetry electrochemical analysis. The simulated molecular docking results indicated that hydrophobic forces were involved in the interaction of BSA with CGA. By studying the interaction mechanism between CGA and BSA, the *in vivo* storage and transport mechanism of CGA under simulated human environment and temperature conditions was elucidated.[16] Therefore, studying the models of

[a]*College of Life Science, Xinyang Normal University, Xinyang, 464000, China. E-mail: toxuwei1986@163.com; xuwei@xynu.edu.cn*

[b]*College of Food and Bioengineering, Henan University of Science and Technology, Luoyang, 471023, China*

interaction and types of forces between TA and proteins at the molecular level may help us to understand their relationship more rationally in order to adjust and improve the structure of the diet.

In this study, the interaction mode and binding mechanism between TA and BSA were studied. The fluorescence quenching mechanisms of TA and BSA were characterized by fluorescence spectroscopy, and their interaction types were elucidated using thermodynamic analysis and calculations. Circular dichroism and differential scanning calorimetry are also used to provide information on relevant protein secondary structure changes and complex properties. Finally, molecular docking simulations were used to understand the amino acid binding sites and docking energies of the interactions between TA and BSA. In order to provide insights into the interaction mechanism between proteins and polyphenols at the molecular level, also provide a theoretical basis for the design and development of TA functional food.

2 Materials and methods

2.1 Materials

Tannin acid (1701.20 g mol^{-1}) was purchased from National Medicine Group Chemical Reagent Co., Ltd (Shanghai, China). Bovine serum albumin (90–120 mg mL^{-1}) was obtained from Sigma-Aldrich Trading Co., Ltd (Shanghai, China). Both sodium dihydrogen phosphate and disodium hydrogen phosphate were supported by National Medicine Group Chemical Reagent Co., Ltd (Shanghai, China). Other chemicals were reagent grade and used without purification. All the solutions used in the experiments were prepared using ultrapure water through a Millipore (Millipore, Milford, MA, USA) Milli-Q water purification system.

2.2 Preparation

The disodium hydrogen phosphate solution and sodium dihydrogen phosphate solution were mixed and adjusted pH = 7 to obtain 0.01 mol L^{-1} phosphate buffer solution (PBS). A certain amount of TA was weighed and added to PBS under light-proof conditions to prepare a TA solution with a concentration of 4×10^{-3} mol L^{-1}. BSA solution was prepared by adding BSA to PBS and shaking gently to prepare a concentration of 8×10^{-6} mol L^{-1}. TA solution and BSA solution were mixed in the volume ratio of 0 : 1, 0.1 : 1, 0.2 : 1, 0.3 : 1, 0.4 : 1, 0.5 : 1, 0.6 : 1, 0.7 : 1, 0.8 : 1, 0.9 : 1, 1.0 : 1 to obtain the mixed solution of TA and BSA.

2.3 Fluorescence spectroscopy

To confirm the interaction between TA and BSA, the fluorescence spectra of BSA with the increasing concentration of TA were determined at 298 K on an RF-5301PC type fluorescence spectrophotometer (Shimadzu, Japan). The excitation wavelength was 280 nm and the emission spectrum was recorded in the range of 290 nm to 450 nm. The fluorescence intensity of the solution to be measured was scanned through a slit of 2.5 nm at a rate of 240 nm min^{-1}. In order to study the type of fluorescence quenching, it is necessary to determine the fluorescence quenching constant as a function of temperature. In this study, the fluorescence quenching spectra of BSA were investigated at three temperatures (298 K, 303 K and 313 K) with increasing TA concentration.[17]

2.4 Fluorescence quenching mechanism

The fluorescence absorption spectra of TA and BSA showed that tannins have a fluorescence quenching effect on BSA. There were two types of fluorescence quenching: dynamic quenching and static quenching. To study the type of fluorescence quenching of TA on BSA, the Stern–Volmer equation can be used to determine the quenching constants at different temperatures.[18] The relationship between temperature and quenching constants can be used to determine the type of quenching that occurs when TA interacts with BSA.

If the BSA molecules quenching is a dynamic quenching due to effective molecular collisions, the Stern–Volmer equation should be satisfied.

$$F_0/F = 1 + K_{sv}[Q] \quad (1)$$

$$K_{sv} = k_q\tau_0 \quad (2)$$

F_0 and F are the fluorescence intensity values before and after TA addition, respectively, k_q is the fluorescence quenching rate constant, τ_0 is the average lifetime of fluorescent molecules without TA addition ($\sim 10^{-8}$ s), $[Q]$ is the TA concentration; K_{sv} is the quenching constant.

2.5 The binding constants and binding sites

Static quenching occurs when TA and BSA react to form complexes. For static quenching, the number of binding sites n and the binding constant K can be derived from the following double logarithmic equation.[19,20]

$$\log[(F_0 - F)/F] = \log K + n\log[Q] \quad (3)$$

F_0 and F are the fluorescence intensity of BSA without and after TA addition, respectively, $[Q]$ is the TA concentration (mol L^{-1}), K is the binding constant, n is the binding site.

2.6 Calculation of thermodynamics

The thermodynamic parameters of the reaction of TA and BSA molecules can be calculated by an equation representing the chemical equilibrium constant *versus* temperature. The enthalpy change of the reaction can be regarded as a constant value when the temperature does not change much. The enthalpy changes of the reaction ΔH, the Gibbs free energy change ΔG and the entropy change ΔS can be calculated from Van't Hoff equation.[21]

$$\ln K_2/K_1 = \Delta H(1/T_1 - 1/T_2)/R \quad (4)$$

$$\Delta G = \Delta H - T\Delta S = -RT\ln K \quad (5)$$

T is the thermodynamic temperature, R is the gas constant (8.314 J (mol^{-1} K^{-1})); K is the binding constant of TA and BSA at the corresponding temperature.

2.7 Circular dichroism

Circular dichroism of the liquid mixture of TA and BSA was measured by a JASCO-type circular dichroism spectrometer (Tokyo, Japan). The parameters were set as a sweep wavelength of 180 ~ 260 nm and a sweep speed of 50 nm min^{-1}. The effect of TA and BSA interaction on the secondary structure of BSA can be determined by observing the circular dichroic chromatogram of the liquid to be measured.[22]

2.8 Differential scanning calorimetry

Differential scanning calorimetry (DSC) experiments were carried out using the TA DSC Q2000 (TA Instruments, USA). Differential scanning calorimetry (DSC) analysis is performed by heating the sample at 3 °C min^{-1} from 10 °C to 100 °C under a nitrogen atmosphere in an open aluminum crucible in a Q2000 instrument connected to a TA 5000 data station and then cooling it to room temperature, a process that is cycled twice.[23]

2.9 Molecular docking

Molecular docking are commonly used to analyze the structure of proteins, the mode of interaction between ligands and proteins and the type of binding sites and forces.[24] The TA structure was first processed using Chemidraw 14.0, then the 3D form of the BSA was obtained from the PDB database. The BSA structure was processed using Mgtools 1.5.6, and finally, the results were derived by Vina manipulation.[25,26] Data analysis was carried out using the Autodock program, using the Lamarckian genetics algorithm and 100 operations to derive the binding sites and the types of forces involved in the interaction between TA and BSA flexibly.

3 Results and discussion

3.1 Effect of TA on the fluorescence spectrum of BSA

Fluorescence spectroscopy is a common method for studying receptor-ligand interactions and is widely used because of its convenience, efficiency and sensitivity. Based on the results of fluorescence spectroscopy, the binding mode and type of binding of receptor and ligand molecules can be further determined. Fig. 1a–c showed the fluorescence spectra at 298 K, 303 K and 313 K, respectively. There was a wave peak of BSA around 342 nm, which indicated that the tryptophan residue was the main source of BSA fluorescence intensity.[27] When TA was added, the fluorescence intensity of BSA decreased significantly, which indicated that TA had a fluorescence quenching effect on BSA, and the quenching effect had a strong dependence on the amount of TA added. In addition, the fluorescence spectrum of BSA shifted slightly red from 342.0 nm to 345.2 nm with a gradual increase in TA concentration. This indicated an interaction between TA and BSA, where the protein peptide chain became stretched and the Trp and Tyr residues buried in the protein interior were exposed to a more hydrophilic environment.[28–30]

3.2 Analysis of fluorescence quenching types

The Stern–Volmer plot of TA and BSA interactions was drawn with $[Q]$ as the horizontal coordinate and F_0/F as the vertical coordinate. To study the type of fluorescence quenching, the fluorescence quenching constants as a function of temperature were determined. According to the obtained $F_0/F - [Q]$ relationship graph, the quenching constants K_{sv} at different temperatures were found using eqn (1) and (2) respectively, an K_{sv} is the slope of a straight line.[31]

The fluorescence quenching constant is the key data to determine the dynamic and static quenching between molecules. For dynamic quenching, as the temperature increases, molecular collisions accelerate, resulting in faster dynamic quenching rates and increased quenching constants, as evidenced by the rise in the slope of the Stern–Volmer line. While for static quenching, the temperature increases, and the explosion constant decreases. The value of the quenching rate constant k_q for dynamic quenching generally defaults to no more than 2.0×10^{10} L (mol^{-1} s^{-1}). In Table 1, the value of K_{sv} decreased from 1.36×10^5 to 1.07×10^5 as the temperature increased from 298 K to 313 K. The slope of the straight line in Fig. 1d similarly reduced with increasing temperature, indicating that the type of fluorescence quenching of TA on BSA was a static quenching rather than a dynamic quenching.[32,33] At 298 K, 303 K and 313 K, the fluorescence quenching rate constant k_q was much larger than the maximum dynamic quenching constant (2.0×10^{10} L (mol^{-1} s^{-1})), this result indicates that TA and BSA play an important role in the binding of them in a static quenching mode as a base-state stable complex.[34,35] Therefore, it is suggested that the interaction mode of TA with BSA is static quenching.

3.3 Calculation of binding constants and binding sites

The bilogarithmic plot of the quenching of BSA by TA at different temperatures according to eqn (3) above was shown in Fig. 1e, where the slope and intercept of the line are positively correlated with the temperature change. The slope is the number of binding sites n and the intercept indicates the binding constant K. The number of binding sites n and the binding constant K are calculated using eqn (3).[36]

As can be seen from Table 2, the binding constant of TA and BSA molecules at 298 K was 2584.64 L mol^{-1}, but when the temperature rose to 303 K the binding constant rose to 20 994.72 L mol^{-1}. The K value of BSA increased with increasing temperature, which indicated that the reaction of BSA with TA was a heat-absorbing reaction, and increasing the temperature was favorable for the stability of the BSA–TA complex. At 298, 303 K and 313 K, the n-values of BSA approximated to a single binding site, which indicated that BSA and TA could form a stable static complex with a 1 : 1 material to quantity ratio.

3.4 Determination of thermodynamic parameters and types of forces

The types of forces that interact between substances include van der Waals force, hydrogen bonding, electrostatic interaction

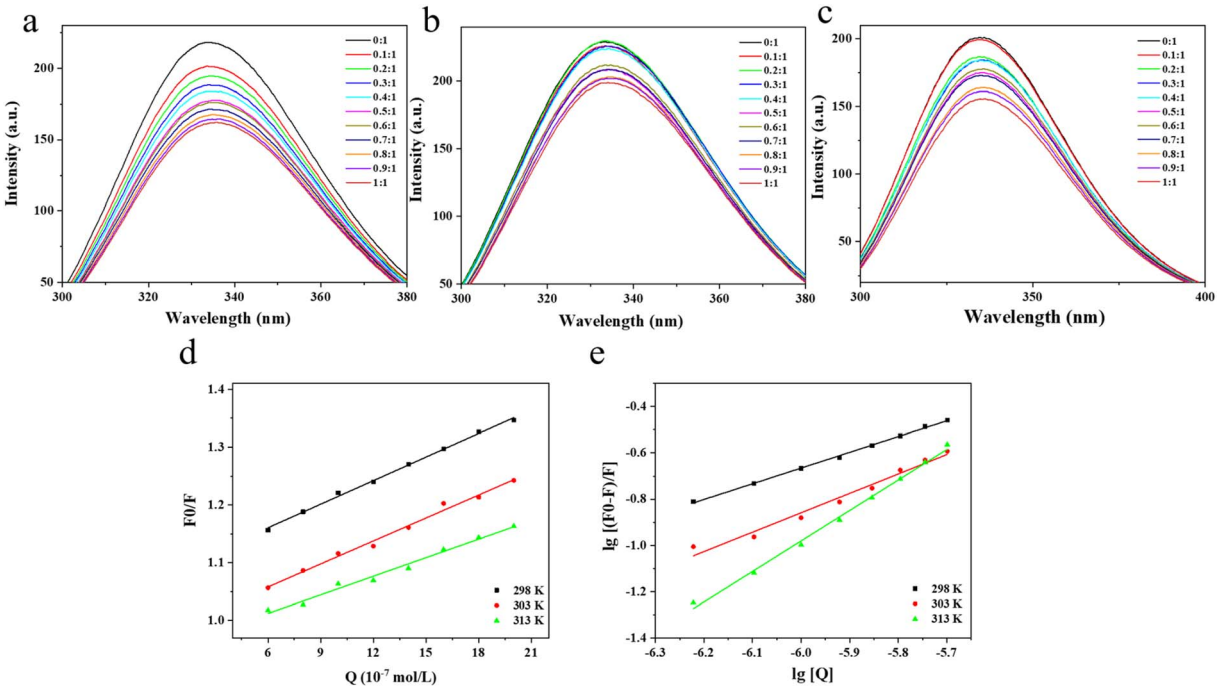

Fig. 1 The interactions between tannin and albumin. Fluorescence spectra of TA–BSA interactions at different temperatures: (a) 298 K, (b) 303 K, (c) 303 K; (d) Stern–Volmer diagram of fluorescence quenching of BSA by TA; (e) double logarithmic curves of BSA quenched by TA at different temperatures.

Table 1 Interaction constants of TA and BSA at different temperatures

T/K	K_{sv} ($\times 10^5$ L mol^{-1})	K_q ($\times 10^{13}$ L mol^{-1} s^{-1})	R^2
298	1.36 ± 0.11	1.36 ± 0.11	0.9964
303	1.33 ± 0.05	1.33 ± 0.05	0.9541
313	1.07 ± 0.06	1.07 ± 0.06	0.9675

Table 2 Binding constant and number of binding sites of TA and BSA at different temperatures

T/K	K (L^{-1} mol^{-1})	n	R^2
198	2584.64 ± 1.22	0.6796 ± 0.11	0.998
303	20 994.72 ± 15.31	0.8567 ± 0.23	0.977
313	26 760.86 ± 15.75	0.8823 ± 0.19	0.995

force and hydrophobic force. When both ΔH and ΔS are greater than zero, the main interaction force is the hydrophobic force. When both are less than zero, it corresponds to hydrogen bonding and van der Waals force. When $\Delta H < 0$ and $\Delta S > 0$, the force is electrostatic gravitational. When $\Delta H > 0$ and $\Delta S < 0$, the intermolecular force is mainly electrostatic gravitational and hydrophobic. The type of forces between BSA and TA can be determined by the change in thermodynamic parameters before and after the reaction.[37]

The thermodynamic parameters of BSA and TA molecules can be calculated by bringing the data in Table 1 into eqn (4) and (5). As seen from Table 3, all ΔG values are negative, indicating that the binding of BSA to TA is a spontaneous process. ΔH and ΔS values for BSA are positive, indicating that hydrophobic forces play a key role in the binding of BSA to TA.

3.5 Effect of TA on circular dichroism of BSA

Circular dichroism is a commonly used method for determining the secondary structure of proteins,[38] which takes advantage of the circular dichroism characteristic of optically active structures in proteins to investigate the effect of TA on the conformation of BSA molecules further. The results of the experiments were shown in Fig. 2a.

The CD spectrum of the TA–BSA interaction had three peaks at 190 nm (+), 208 nm (−) and 222 nm (−), which were consistent with the circular dichroism characteristic of the α-helix. It proved the presence of the α-helix in BSA.[39] The CD spectra of the interaction between BSA and TA changed with increasing TA concentration, which indicated that TA interacted with the BSA molecule and changed the secondary structure of the BSA molecule. The CD spectroscopic data showed that helices and irregular curls were the main secondary structures of BSA in the absence of TA. With the

Table 3 Thermodynamic parameters of TA and BSA binding at different temperatures

T/K	ΔG (kJ mol^{-1})	ΔH (kJ mol^{-1})	ΔS (kJ mol^{-1})
298	−19.4671	85.66	0.352776
303	−25.0706		0.082741
313	−26.5295		0.084759

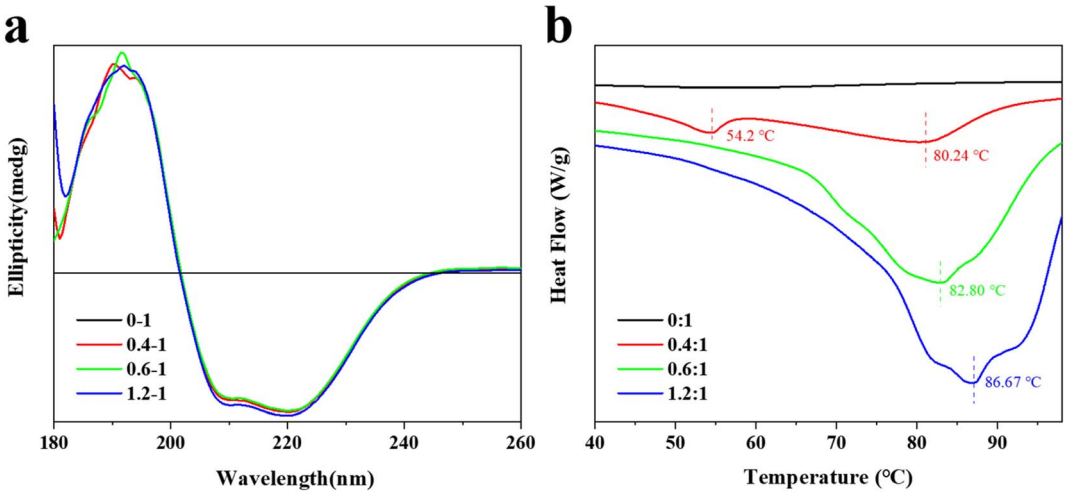

Fig. 2 Circular dichroism and differential scanning calorimetry. (a) Circular dichroism of the interaction between TA and BSA; (b) differential scanning calorimetry of the interaction between TA and BSA.

increase of TA content, the α-helix in the BSA molecule remained basically at 25.70%. Interestingly, when the TA to BSA molar ratio reached 1.2 : 1, the α-helix rose by 0.3%. Similarly, in the absence of TA, the amount of irregular curl of BSA molecules was 37.5%, which decreased to 37.1% when the molar ratio of TA to BSA was 1.2 : 1. However, with the increase of TA, the content of β-corner remained unchanged at 18.4%. This indicates that the secondary structure of the BSA molecules changed as the TA content increased, which suggests an interaction between them.[40] This result is consistent with the results of fluorescence spectroscopy.

3.6 Differential scanning calorimetry of TA and BSA

The differential scanning calorimetric analysis curves of the interaction between BSA and different contents of TA are shown in Fig. 2b. The melting curve of BSA without TA is smooth with a melting temperature of 24.12 °C and an enthalpy of 109.6 J

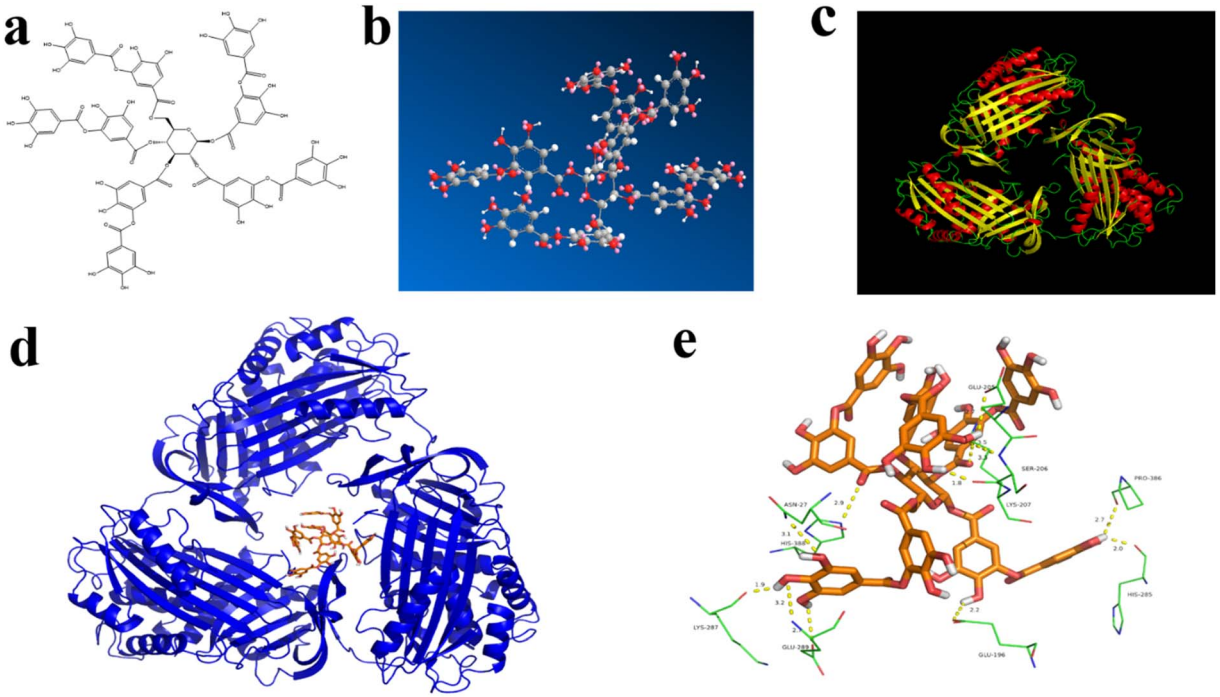

Fig. 3 Molecular docking. (a) The molecular structure of TA; (b) ball-and-stick model of the TA molecule; (c) the crystal three-dimensional structure of BSA molecule; (d) simulation of the three-dimensional structure of TA and BSA binding; (e) schematic diagram of the tannin-albumin interaction site.

g^{-1}. Compared with the differential scanning calorimetric analysis curve of BSA without TA, there are two heat absorption peaks when the ratio of TA to BSA is 0.4 : 1, which are the water loss peak and the melting peak. The melting curve was smooth when the ratio of TA to BSA was 0.4 : 1, with a melting temperature of 80.24 °C and an enthalpy of 285.1 J g^{-1}. In contrast, only one melting peak existed when the ratio of TA to BSA was 0.6 : 1, indicating that BSA and TA had formed a homogeneous complex by self-assembly, which was consistent with the results of fluorescence spectrum. The interaction between BSA and TA improves the stability of both, so that the melting temperature increases to 86.67 °C and the enthalpy increases to 264.1 J g^{-1} when the ratio of TA to BSA is 1.2 : 1.[41] This is consistent with the result of thermodynamic calculation.

3.7 TA and BSA molecular docking analysis

Molecular docking is an effective method for molecular interaction analysis and can provide more information about the interaction between TA and BSA. Therefore, molecular docking was used to investigate the effects of TA–BSA interactions further. Fig. 3a and b showed the molecular structure of TA. The TA molecule has many hydroxyl groups, and oxygen and hydrogen on the hydroxyl groups can form hydrogen bonds. As shown in Fig. 3c, the energy-optimal conformation was selected by analyzing the results of Vina pairs. The analysis of the active site showed that the active site of BSA is located between the helix and the convolution, and the small molecule ligands may act on this active site. Fig. 3d and e simulate the combined conformation of TA and BSA. TA mainly enters the active site of BSA target protein through hydrophobic and van der Waals forces. There are many hydroxyl groups on TA, and oxygen and hydrogen on the hydroxyl group can form hydrogen bonds. It mainly forms hydrogen bond interactions with amino acid residues at the active site of BSA, such as ASN 27, LYS 287, PRO 386, GLU 196, GLU 205, SER 206, LYS 207, HIS 285 and HIS 388. The TA binding conformation to the BSA target protein was simulated by molecular docking with a docking energy of −12.9 kcal mol^{-1} to non-covalently bind the protein active site.

4 Conclusion

In this study, fluorescence spectroscopy, circular dichroism, differential scanning calorimetry analysis and molecular docking were used to evaluate BSA–TA interactions. The fluorescence spectroscopy data showed that BSA and TA underwent static quenching and formed complexes mainly by hydrophobic forces spontaneously bonding at a substance-to-matter ratio of 1 : 1 and causing a decrease in the hydrophobicity of the BSA surface. In addition, the circular dichroism study also detected the secondary structure change of BSA with the increase of TA content, which mainly showed the increase of α-helix and the decrease of random curl. And differential scanning calorimetry analysis showed that the interaction between BSA and TA improved the stability of both. The results of molecular docking clearly measured the binding sites of BSA and TA with a docking energy of −12.9 kcal mol^{-1} to the active site in the form of non-covalent bonds. This study explored the mechanism of TA–BSA interactions and provided useful theoretical support for understanding the binding properties and interactions between proteins and bioactive molecules. In addition, these findings open up the possibility of BSA-based food formulations as effective carriers of multiple bioactive nutrients.

Author contributions

Wei Xu: supervision, writing-review. Yuli Ning: investigation, methodology, writing – original draft. Shiwan Cao: resources, conceptualization, data curation. Guanchen Wu: formal analysis. Haomin Sun: conceptualization, supervision, writing – review & editing. Liwen Chai: methodology. Shuping Wu: data curation, writing – original draft. Jingyi Li: methodology. Denglin Luo: validation, writing and review. Bakht Ramin Shah: validation, writing and review.

Conflicts of interest

No conflict of interest exits in the submission of this manuscript, and manuscript is approved by all authors for publication. Each of the coauthors have seen and agrees with each of the changes made to this manuscript in the revision.

Acknowledgements

This work was financially supported by the National Natural Science Foundation of China (Grant No. U2004160), Natural Science Foundation of Henan (Grant No. 222103810071), University Student Scientific Research Projects of Xinyang Normal University (Grant No. 2021-DXS-114), Innovation and Entrepreneurship Training Programs for College students in Henan Province (Grant No. S202110477040), and Nanhu Scholars Program for Young Scholars of XYNU. This research was also kindly supported by the Analysis Testing Center of Xinyang Normal University.

References

1 J. Lyu, J. Fu, S. Chen, Y. Xu, Y. Nie and K. Tang, Impact of tannins on intraoral aroma release and retronasal perception, including detection thresholds and temporal perception by taste, in model wines, *Food Chem.*, 2022, **375**, 131890.
2 A. Vignault, J. Gombau, M. Jourdes, V. Moine, J. M. Canals, M. Fermaud, *et al.*, Oenological tannins to prevent Botrytis cinerea damage in grapes and musts: kinetics and electrophoresis characterization of laccase, *Food Chem.*, 2020, **316**, 126334.
3 F. Yang, J. Yang, S. Qiu, W. Xu and Y. Wang, Tannic acid enhanced the physical and oxidative stability of chitin particles stabilized oil in water emulsion, *Food Chem.*, 2021, **346**, 128762.
4 H. Li, F. Xu, C. Liu, A. Cai, J. A. Dain, D. Li, *et al.*, Inhibitory effects and surface plasmon resonance-based binding affinities of dietary hydrolyzable tannins and their gut

microbial metabolites on SARS-CoV-2 main protease, *J. Agr. Food Chem.*, 2021, **69**(41), 12197–12208.

5 H. Pan, Y. Wang, X. Xu, Z. Qian, H. Cheng, X. Ye, *et al.*, Simultaneous extraction and depolymerization of condensed tannins from Chinese bayberry leaves for improved bioavailability and antioxidant activity, *J. Agr. Food Chem.*, 2021, **69**(38), 11292–11302.

6 F. Zhan, J. Yang, J. Li, Y. Wang and B. Li, Characteristics of the interaction mechanism between tannic acid and sodium caseinate using multispectroscopic and thermodynamics methods, *Food Hydrocolloids*, 2018, **75**, 81–87.

7 T. Niu, X. Zhu, D. Zhao, H. Li, P. Yan, L. Zhao, *et al.*, Unveiling interaction mechanisms between myricitrin and human serum albumin: insights from multi-spectroscopic, molecular docking and molecular dynamic simulation analyses, *Spectrochim. Acta, Part A*, 2023, **285**, 121871.

8 H. Yang, L. Xu, Y. Liang, Y. Chen, Y. Li, X. Fan, *et al.*, A "traffic jam" of (+)-catechin caused by hyperglycemia—The interaction between (+)-catechin and human serum albumin (HSA) in high glucose environment, *J. Mol. Liq.*, 2022, **355**, 118975.

9 N. Rahman and N. Khalil, Effect of glycation of bovine serum albumin on the interaction with xanthine oxidase inhibitor allopurinol: Spectroscopic studies and molecular modeling, *J. Mol. Liq.*, 2022, **367**, 120396.

10 K. N. Deepa, S. Nawsheen, M. A. Sufian and S. A. Islam, In-vitro Fluorescence Spectroscopic Analysis of the Interaction of Glimepiride with Bovine Serum Albumin (BSA), *J. Pharm. Res. Int.*, 2019, **30**, 2456–9119.

11 Z. Tian, L. Tian, M. Shi, S. Zhao, S. Guo, W. Luo, *et al.*, Investigation of the interaction of a polyamine-modified flavonoid with bovine serum albumin (BSA) by spectroscopic methods and molecular simulation, *J. Photochem. Photobiol., B*, 2020, **209**, 111917.

12 Y. C. Luo and P. Jing, Molecular Interaction of Protein-Pigment C-Phycocyanin with Bovine Serum Albumin in a Gomphosis Structure Inhibiting Amyloid Formation, *Int. J. Mol. Sci.*, 2020, **21**(21), 8207.

13 E. Fliszár-Nyúl, B. Lemli, S. Kunsági-Máté, L. Dellafiora, C. Dall'Asta, G. Cruciani, *et al.*, Interaction of mycotoxin alternariol with serum albumin, *Int. J. Mol. Sci.*, 2019, **20**(9), 2352.

14 Y. Lv, Q. Liang, Y. Li, X. Liu, D. Zhang and X. Li, Study of the binding mechanism between hydroxytyrosol and bovine serum albumin using multispectral and molecular docking, *Food Hydrocolloids*, 2022, **122**, 107072.

15 J. Zhao, L. Huang, R. Li, Z. Zhang, J. Chen and H. Tang, Multispectroscopic and computational evaluation of the binding of flavonoids with bovine serum albumin in the presence of Cu^{2+}, *Food Chem.*, 2022, **385**, 132656.

16 W. Jia, X. Jin, W. Liu, B. Zhao, M. Zhang, Y. Yang, *et al.*, Evaluation the binding of chlorogenic acid with bovine serum albumin: spectroscopic methods, electrochemical and molecular docking, *Spectrochim. Acta, Part A*, 2023, **291**, 122289.

17 F. Zhan, S. Ding, W. Xie, X. Zhu, J. Hu, J. Gao, *et al.*, Towards understanding the interaction of β-lactoglobulin with capsaicin: multi-spectroscopic, thermodynamic, molecular docking and molecular dynamics simulation approaches, *Food Hydrocolloids*, 2020, **105**, 105767.

18 B. Zhang, J. Zhang, X. Yu, J. Peng, L. Pan and K. Tu, Evaluation of the adsorption capacity and mechanism of soy protein isolate for volatile flavor compounds: role of different oxygen-containing functional groups, *Food Chem.*, 2022, **386**, 132745.

19 D. P. Ašanin, S. Skaro Bogojevic, F. Perdih, T. P. Andrejević, D. Milivojevic, I. Aleksic, *et al.*, Structural characterization, antimicrobial activity and BSA/DNA binding affinity of new silver (I) complexes with thianthrene and 1,8-naphthyridine, *Molecules*, 2021, **26**(7), 1871.

20 M. Rubio Camacho, J. A. Encinar, M. J. Martínez-Tomé, R. Esquembre and C. R. Mateo, The interaction of temozolomide with blood components suggests the potential use of human serum albumin as a biomimetic carrier for the drug, *Biomolecules*, 2020, **10**(7), 1015.

21 N. Baranov, S. Racovita, S. Vasiliu, A. M. Macsim, C. Lionte, V. Sunel, *et al.*, Immobilization and release studies of triazole derivatives from grafted copolymer based on gellan-carrying betaine units, *Molecules*, 2021, **26**(11), 3330.

22 C. Jia, D. Cao, S. Ji, X. Zhang and B. Muhoza, Tannic acid-assisted cross-linked nanoparticles as a delivery system of eugenol: the characterization, thermal degradation and antioxidant properties, *Food Hydrocolloids*, 2020, **104**, 105717.

23 L. Ferron, C. Milanese, R. Colombo and A. Papetti, Development of an accelerated stability model to estimate purple corn cob extract powder (Moradyn) shelf-life, *Foods*, 2021, **10**(7), 1617.

24 Z. Guo, Y. Huang, J. Huang, S. Li, Z. Zhu, Q. Deng, *et al.*, Formation of protein-anthocyanin complex induced by grape skin extracts interacting with wheat gliadins: Multi-spectroscopy and molecular docking analysis, *Food Chemistry*, 2022, **385**, 132702.

25 J. E. Dolatabadi, V. Panahi Azar, A. Barzegar, A. A. Jamali, F. Kheirdoosh, S. Kashanian, *et al.*, Spectroscopic and molecular modeling studies of human serum albumin interaction with propyl gallate, *RSC Adv.*, 2014, **4**(110), 64559–64564.

26 M. Sharifi, J. E. Dolatabadi, F. Fathi, M. Rashidi, B. Jafari, H. Tajalli, *et al.*, Kinetic and thermodynamic study of bovine serum albumin interaction with rifampicin using surface plasmon resonance and molecular docking methods, *J. Biomed. Opt.*, 2017, **22**(3), 037002.

27 B. Demoro, A. Bento Oliveira, F. Marques, J. Costa Pessoa, L. Otero, D. Gambino, *et al.*, Interaction with blood proteins of a ruthenium (II) nitrofuryl semicarbazone complex: Effect on the antitumoral activity, *Molecules*, 2019, **24**(16), 2861.

28 S. C. Gaglio, M. Donini, P. E. Denbaes, S. Dusi and M. Perduca, Oxyresveratrol inhibits R848-induced pro-inflammatory mediators release by human dendritic cells

even when embedded in PLGA nanoparticles, *Molecules*, 2021, **26**(8), 2106.

29 J. Jiang, Z. Zhang, J. Zhao and Y. Liu, The effect of non-covalent interaction of chlorogenic acid with whey protein and casein on physicochemical and radical-scavenging activity of in vitro protein digests, *Food Chem.*, 2018, **268**, 334–341.

30 X. Sun, H. N. Ferguson and A. E. Hagerman, Conformation and aggregation of human serum albumin in the presence of green tea polyphenol (EGCg) and/or palmitic acid, *Biomolecules*, 2019, **9**(11), 705.

31 C. M. Castillo Fraire, E. Brandão, P. Poupard, J. M. Le Quére, E. Salas, V. Freitas, *et al.*, Interactions between polyphenol oxidation products and salivary proteins: Specific affinity of CQA dehydrodimers with cystatins and PB peptide, *Food Chem.*, 2021, **343**, 128496.

32 N. A. Alsaif, A. A. AlMehiziaa, A. H. Bakheit, S. Zargar and T. A. Wani, A spectroscopic, thermodynamic and molecular docking study of the binding mechanism of dapoxetine with calf thymus DNA, *S. Afr. J. Chem.*, 2020, **73**(1), 44–50.

33 T. A. Wani, N. Alsaif, A. H. Bakheit, S. Zargar, A. A. AlMehizia and A. A. Khan, Interaction of an abiraterone with calf thymus DNA: Investigation with spectroscopic technique and modelling studies, *Biorg. Chem.*, 2020, **100**, 103957.

34 H. Shen, J. Wang, J. Ao, Y. Cai, M. Xi, Y. Hou, *et al.*, Inhibitory kinetics and mechanism of active compounds in green walnut husk against α-glucosidase: Spectroscopy and molecular docking analyses, *LWT–Food Sci. Technol.*, 2022, **172**, 114179.

35 H. Wang, H. Zhang, Q. Liu, X. Xia, Q. Chen and B. Kong, Exploration of interaction between porcine myofibrillar proteins and selected ketones by GC-MS, multiple spectroscopy, and molecular docking approaches, *Food Res. Int.*, 2022, **160**, 111624.

36 L. Wang, L. Wang, T. Wang, Z. Li, Y. Gao, S. W. Cui, *et al.*, Comparison of quercetin and rutin inhibitory influence on Tartary buckwheat starch digestion in vitro and their differences in binding sites with the digestive enzyme, *Food Chem.*, 2022, **367**, 130762.

37 J. Zheng, C. H. Tang, G. Ge, M. Zhao and W. Sun, Heteroprotein complex of soy protein isolate and lysozyme: Formation mechanism and thermodynamic characterization, *Food Hydrocolloids*, 2020, **101**, 105571.

38 Y. Lu, R. Zhao, C. Wang, X. Zhang and C. Wang, Deciphering the non-covalent binding patterns of three whey proteins with rosmarinic acid by multi-spectroscopic, molecular docking and molecular dynamics simulation approaches, *Food Hydrocolloids*, 2022, **132**, 107895.

39 V. S. Mandala, S. Y. Liao, M. D. Gelenter and M. Hong, The Transmembrane conformation of the influenza B virus M2 protein in lipid bilayers, *Sci. Rep.*, 2019, **9**(1), 3725.

40 L. Zhang, Y. Liu, X. Hu, M. Xu and Y. Wang, Studies on interactions of pentagalloyl glucose, ellagic acid and gallic acid with bovine serum albumin: a spectroscopic analysis, *Food Chemistry*, 2020, **324**, 126872.

41 M. Huang, Y. Song, N. Lv, C. Liu, G. Ren, Q. Shen, *et al.*, Theoretical and experimental perspectives of interaction mechanism between zein and lysozyme, *Food Hydrocolloids*, 2022, **132**, 107876.